Analyst

PAPER

View Article Online
View Journal | View Issue

Cite this: *Analyst*, 2017, **142**, 4247

The influence of covalent immobilization conditions on antibody accessibility on nanoparticles†

Bedabrata Saha, ‡[a] Pål Songe,[b] Toon H. Evers[a] and Menno W. J. Prins *§[a,c]

The accessibility of particle-coupled antibodies is important for many analytical applications, but comprehensive data on parameters controlling the accessibility are scarce. Here we report on the site-specific accessibility of monoclonal antibodies, immobilized on magnetic nanoparticles (500 nm) by the widely used covalent EDC coupling method, with the variation of four key coupling parameters (surface activation and immobilization pH, crosslinker and antibody concentration ratios). By developing quantitative radio-labelled assays, the number of immobilized antibodies, the Fab domain accessibility (in a sandwich immunoassay), and the Fc domain accessibility (in a Protein G assay) were determined. For sub-monolayer surface coverage, the observed numbers of accessible Fab and Fc domains are equal and scale linearly with the antibody density. For above monolayer coverage, the fractions of accessible Fab and Fc domains decrease, in an unequal manner. The results show that the antibody accessibility is primarily determined by the antibody surface density, rather than by chemical reactivity or the charge state, and that crowded conditions affect Fab and Fc accessibility in an unequal manner.

Received 28th August 2017,
Accepted 28th September 2017

DOI: 10.1039/c7an01424d

rsc.li/analyst

Introduction

The ability of antibodies to bind to target proteins at solid–liquid interfaces is at the core of many *in vitro* diagnostic assays and *in vivo* therapeutics. The activity of an immobilized antibody, *i.e.* its target binding capability, finds its origin in its Fab domain that is (i) accessible, *i.e.* has an outward orientation from the interface, and (ii) is biologically active, *i.e.* has a molecular conformation with a low dissociation constant (K_d) for the target molecule. The target-binding activity of antibodies immobilized at a solid–liquid interface has been studied as a function of immobilization strategy, molecular orientation, surface crowding of the antibodies, and solid surface properties.[1–4] It has been established that the activity of immobilized antibodies varies sensitively between different immobilization chemistries and that antibodies with more accessible Fab domains exhibit higher activity than randomly immobilized antibodies.[5–7] However, data on how the accessibility of antibodies depends on the chemical coupling conditions within a given immobilization strategy are scarce and the underlying mechanisms are not yet well understood.

On planar surfaces, several techniques[8–12] have been used to determine the activity, accessibility and orientation of immobilized antibodies: atomic force microscopy,[8,9] neutron reflection,[10] spectroscopic ellipsometry[11] and mass spectrometry,[12] with focus on the quantification of the immobilized layer thickness and density. From these studies, the picture arises that non-directional coupling on planar surfaces yields predominantly side-on oriented antibodies at low densities, and more end-on orientation at high densities. The molecular arrangement of antibodies at higher concentrations leads to a tightly packed antibody layer with a heterogeneous distribution of orientations.[10,11]

On nanoparticles, the abovementioned experimental methods are not well applicable, so other techniques have been developed.[13–16] The activity and accessibility of antibodies on nanoparticles have been studied for example by enzyme activity mediated colorimetric assays[13,14] and magnetic particle based sandwich optical and electrochemical assays.[14,15] However, these techniques do not give precise quantitative information and the studies were not focused on an in-depth understanding of the influence of immobilization parameters. In a previous paper,[16] we have developed a

[a]*Philips Research, High Tech Campus, 5656 AE Eindhoven, The Netherlands*
[b]*Thermo Fisher Scientific, 0379 Oslo, Norway*
[c]*Department of Biomedical Engineering, Department of Applied Physics, and Institute for Complex Molecular Systems, Eindhoven University of Technology, 5600 MB Eindhoven, The Netherlands. E-mail: m.w.j.prins@tue.nl*

†Electronic supplementary information (ESI) available: Detailed experimental section, characterization of radio-labelling of biomolecules, additional analysis of site-specific accessibility assays. See DOI: 10.1039/c7an01424d

‡Zoetis Denmark ApS, Gammelgårdsvej 87C, 3520, Farum, Denmark.
§Eindhoven University of Technology, Eindhoven, The Netherlands.

supernatant immunoassay to study the Fab domain activity of nanoparticle-coupled anti-troponin antibodies, which showed a decrease of antigen-capturing activity around monolayer coverage, studied for a single chemical coupling condition.

Here, we address the question how covalent chemical coupling conditions influence the Fab domain as well as the Fc domain accessibility of nanoparticle-coupled antibodies, quantified over a broad range of antibody surface densities using radio-labelled assays. *In situ* accessibility and orientation is a key factor as it directly relates to the immobilized antibody activity for capturing biomarkers and further performances in affinity-based assays. We studied the dependencies of covalent antibody immobilization using the hetero-crosslinker 1-ethyl-3-(3-dimethylaminopropyl)carbodiimide (EDC), which provides a stable bond between a carboxyl group on one end and a primary amine on the other end. Among the covalent immobilization strategies,[17,18] the immobilization strategy with EDC was chosen because of its extensive use in biofunctionalization for research and commercial purposes, due to its robustness and minimal need for chemical modification.

Monoclonal anti-troponin antibodies were covalently and non-directionally coupled to magnetic nanoparticles, with the variation of four chemical coupling parameters. Cardiac troponin I is a key biomarker for the diagnosis of myocardial infarction;[19] hence it is very relevant for applications in rapid diagnostic testing. The method requires the presence of carboxyl or amine groups on the solid surface. We used 500 nm magnetic nanoparticles with a carboxyl-functionalized polystyrene shell. Superparamagnetic nanoparticles (MNP) are widely applied in diagnostics and bio-separation applications due to their controllable magnetic separation.[20] The rationale behind the chosen coupling parameters is as follows (see also Scheme 1A and Table 1). The carboxyl groups on the nanoparticle surface were activated by the hetero-crosslinker EDC and the excess EDC was washed off. The solution pH of this reaction and the EDC to carboxyl group ratio are important for the intermediate ester bond formation and for the number of activated groups on the particle surface. A higher amount of EDC leads to more activated carboxyl groups which can result in a higher density of immobilized antibodies. Next, antibody molecules were incubated with the surface activated nanoparticles, covalently binding the antibodies to the nanoparticle surface *via* their primary amine groups. The coupling pH controls the charge state of the antibody molecules and thereby the strength of the electrostatic repulsion between deprotonated antibodies and negatively charged surface carboxyl groups, with higher repulsion expected to occur at a higher pH. Finally, the molar ratio of antibody molecules to the total nanoparticle surface area is an important parameter for coupling effectiveness. For reasons of sensitivity and precision, the number of immobilized antibodies and their site-specific accessibility were determined by radio-labelled assays as developed, using antigen (troponin I), antibodies for a sandwich assay, and protein G.

Experimental

Materials

Superparamagnetic carboxylic acid coating (prototype particles, average diameter of 500 nm), with 1 wt% particle concentration in the stock solution (specific surface area 25.0 $m^2\ g^{-1}$), was kindly provided by Thermo Fisher Scientific (former Life Technologies, Oslo, Norway). The density of the carboxylic group on the nanoparticle surface was 0.7 mmol per 1 g of nanoparticles as provided by the supplier. The surface potential (zeta potential) of the nanoparticles at pH 7.4 was −44.2 ± 1.4 mV, as measured using a Malvern Zeta sizer. For zeta-potential measurement, the nanoparticles were diluted to 0.05 wt% in 10 mM phosphate buffer (pH 7.4) and were sonicated briefly before use. Cardiac troponin I (cTnI, in the form of troponin ITC complex, molecular weight 26 kDa) and monoclonal anti-troponin I antibodies mAb1 and mAb2, designed to bind a single cTnI per antibody molecule (mouse IgG, molecular weight 150 kDa), were purchased from Hytest Ltd (Finland). The recombinant protein G molecules (bind to the Fc domain of IgG, without the albumin and cell surface binding domain, molecular weight ~21.6 kDa) in lyophilized form were purchased from Thermo Fisher Scientific (Product No. 21193). The crosslinker EDC [(1-ethyl-3-(3-dimethylaminopropyl)carbodiimide hydrochloride)] was purchased from Thermo Fisher Scientific. The ^{125}I radionuclide (in a stock of 5 mCi/185 MBq, specific activity 17 Ci per mg or 629 GBq per mg), used for labelling of biomolecules, was obtained from PerkinElmer. The iodination tubes for the labelling of biomolecules with ^{125}I were purchased from Thermo Fisher Scientific.

Labelling of proteins with ^{125}I and characterization

The direct radiolabelling of the mAb1, mAb2 and protein G with ^{125}I was carried out using the iodination tubes, coated with an iodination reagent (or 'Iodo-gen': 1,3,4,6-tetrachloro-3α,6α-diphenylglycouril) from Thermo Fisher Scientific (Cat. No. 28601). For each set of labelling experiments, about 2 MBq of radio-labelled ^{125}I was added per 20 μg of proteins (mAb1, mAb2, protein G). Briefly, 20 μg protein solution in phosphate buffer (pH 7.4) was added to the iodination tubes. A diluted stock of the ^{125}I radionuclide was made by adding 0.8 μl of the stock solution to the 50 μl phosphate buffer, pH 7.4 (total activity 12.8 MBq). From this diluted stock, 8 μl was added to 20 μg of protein solution in the iodination tube, and the final volume was made up to 100 μl with phosphate buffer (end concentration of 1.3 μM and 6.4 μM for mAb1/mAb2 and protein G, respectively). The iodination reagent pre-coated tubes can provide efficient labelling compared to the solution-based methods, which involves the much higher possibilities of oxidation. Typically, the sodium iodide was converted to the activated form of iodine by the pre-coated iodination reagent, and subsequently interacted with the certain amino acid side chains, for *e.g.* tyrosine (incorporated into the *ortho* position of the hydroxyl groups of tyrosine) of the protein molecules. The reaction mixture was incubated at room temperature for 15 min

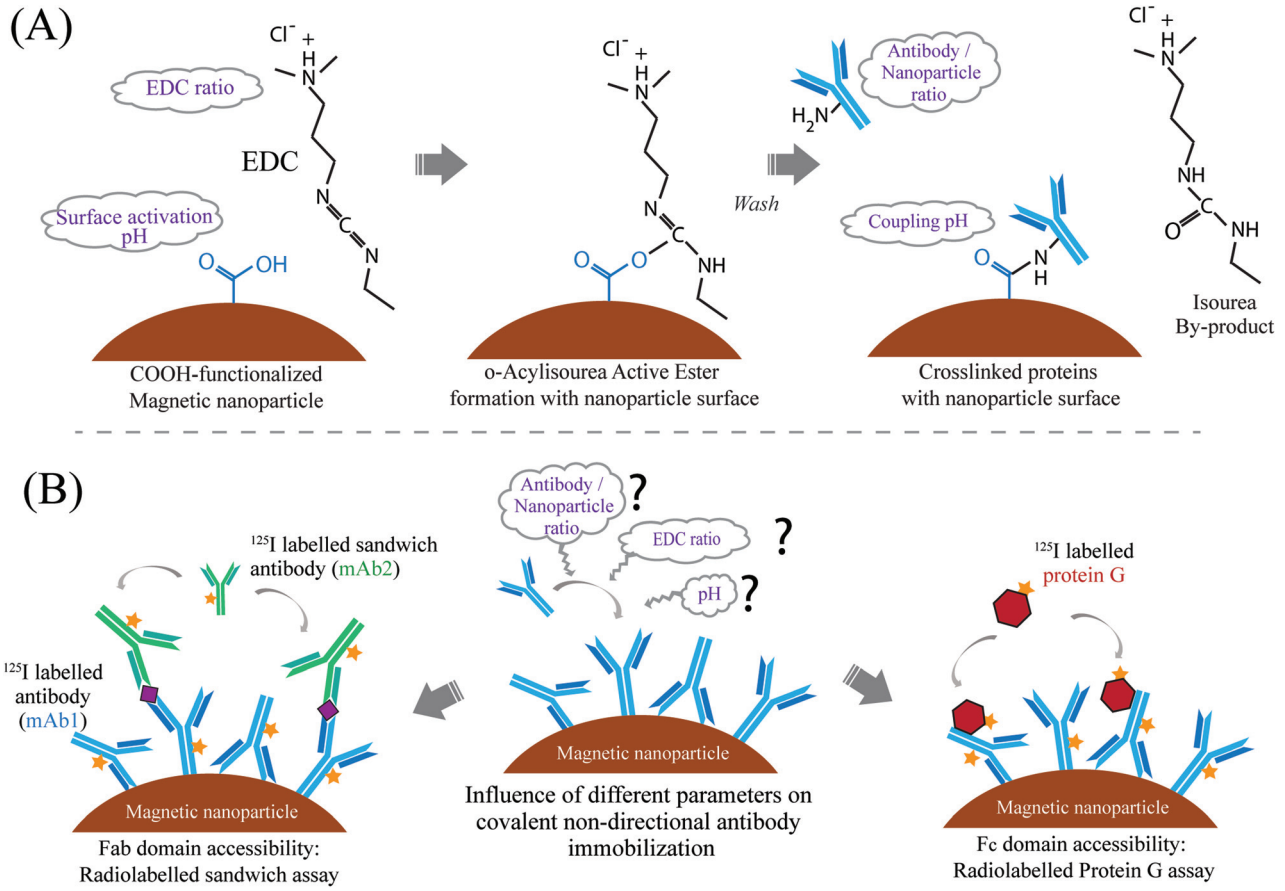

Scheme 1 Schematic representation of the reaction steps and experimental approach. (A) Reaction steps of covalent immobilization of antibody molecules *via* a primary amine on the carboxylic acid-functionalized nanoparticle surface using the hetero-crosslinker EDC. The carboxyl modified nanoparticle surface was first activated with EDC to form an intermediate ester. Furthermore, the antibody molecules were conjugated *via* their surface-exposed primary amines to the nanoparticle surface. Four parameters were varied: EDC to surface carboxyl group ratio, nanoparticle surface activation pH, antibody to nanoparticle surface ratio, and coupling pH. (B) Experimental set up for analyzing the influence of these chemical parameters on immobilization density and site-specific accessibility. Monoclonal anti-troponin antibody (mAb1, ^{125}I labelled) was immobilized with different chemical parameters and quantified. Two different assays were used to analyze the site-specific accessibility of the immobilized antibodies. To quantify the accessibility of the antigen binding site (Fab domain) of the immobilized antibodies, a target molecule capture mediated sandwich assay was used with a second ^{125}I labelled antibody (mAb2). The Fc domain accessibility of the nanoparticle-coupled antibodies was quantified using ^{125}I labelled recombinant protein G (containing the Fc binding domain).

Table 1 Coupling conditions used for the immobilization of mAb1 on magnetic nanoparticles

Parameters	Variation
pH of nanoparticle surface activation buffer (15 mM MES buffer) (pH_a)	pH 5.0–6.0
EDC added to the COOH nanoparticles	0.5–2.0 mol eq. ratio of EDC to COOH groups per 1 mg of nanoparticles
pH of antibody coupling buffer (15 mM MES buffer) (pH_c)	pH 5.5–6.5
Antibody added to nanoparticles (mAb1)	20–100 μg antibody per 1 mg of nanoparticles (0.1–0.6 nmol m^{-2}, and 1.6×10^{-4}–8.1×10^{-4} mol eq. ratio of mAb1/COOH groups on the particle surface)

under continuous stirring. The completion of the reaction was analyzed by thin layer chromatography (TLC) by withdrawing a small volume (~1 μl) of the reaction mixture. The reaction mixture spots on TLC silica plates were analyzed in a phosphoimager (PerkinElmer) for the ^{125}I labelled proteins and free ^{125}I (ESI, Fig. S1†). Furthermore, the labelled proteins were purified by size-exclusion chromatography using a Biosep-SEC-S 3000 column, attached with a radioactive flow detector. Furthermore, the purified labelled proteins were analyzed by SDS-PAGE in homogeneous 7.5% 'Phast Gel' (GE Healthcare). The bands in the SDS-PAGE were scanned in the phosphoimager and optical imaging. Finally, 100% radio-labelled protein solutions were mixed with the same un-labelled protein solutions, to make a homogeneous final solution with a known required concentration. This mixing was needed to work in the detectable range of the Gamma Counter (PerkinElmer). The concentration of this homogeneous solution of labelled and un-labelled proteins was

quantified using a NanoDrop and subsequent radioactivity was measured (from a known concentration solution) in an automatic Gamma Counter.

Immobilization of antibodies (mAb1) on magnetic nanoparticles

The covalent immobilization of anti-troponin I antibody mAb1 on 500 nm magnetic nanoparticles was performed under four different chemical parameters (summarized in Table 1). The antibody coupling experimental design with the variation of these different chemical parameters (*i.e.* activation and coupling pH of 15 mM MES buffer, EDC concentration and mAb1 concentration) was set up using the MODDE design of experiment software. A total of 19 sets of experiments were performed combining different chemical parameters as shown in Table S1 (ESI†). Briefly, the stock nanoparticle solution was washed and buffer exchanged to 15 mM MES buffer (2-(*N*-morpholino)ethanesulfonic acid, pH 6.0), by using magnetic separation. The nanoparticle surface was then activated by adding different concentrations of EDC (*N*-3-(dimethylamino)propyl-*N*-ethylcarbodimide hydrochloride); 0.5 to 2.0 mole equivalent to the COOH groups of nanoparticles), in 15 mM MES buffer of different pH values (pH 5.0 to 6.0). After incubating for 30 min with EDC and washing with MES buffer, different amounts of mAb1 (20–100 μg of mAb1 per mg of nanoparticles or, 0.1–0.6 nmol of mAb1 per 1 m^2 of the available nanoparticle surface area, calculated from the provided specific surface area 25.0 m^2 g^{-1} of the nanoparticles) were added for coupling with nanoparticles in 15 mM MES buffer of different pH values (pH 5.5 to 6.5). The antibody-added nanoparticle solution was incubated at room temperature for 1.5 h, followed by removal of the supernatant by magnetic separation. The unbound COOH groups on the particle surface were further deactivated with 50 mM TBST buffer (Tris buffer saline, 0.05% tween, pH 7.4), by incubating for 30 min and subsequent three time washing with TBST buffer. No additional blocking of the surfaces was performed in order to evaluate only the influence of the EDC conjugation on the accessibility of antibodies. Finally, the mAb1 coupled nanoparticles were stored in TBST buffer at an end concentration of 10 mg ml^{-1}, at 4 °C after brief sonication for further use. The nanoparticle solution was also sonicated briefly after each magnetic separation step, for proper resuspension of the nanoparticles. The loss of particles in several pipetting and magnetic separation steps was negligible. In a later stage of this study, an additional set of coupling experiments were performed with a higher mAb1 concentration (50–500 μg of mAb1 per mg of bead; 6.2×10^3 to 62.2×10^3 mAb1 per nanoparticle), while keeping the other parameter fixed; likely 1.0 mole equivalent EDC, 15 mM MES buffer of pH 5.5 for surface activation and antibody coupling (ESI, Table S2†). The same protocol was followed for this set of experiments as mentioned above.

Quantification of immobilized antibodies (mAb1)

The amount of immobilized mAb1 was directly quantified by measuring the radioactivity of the labelled mAb1 in an automatic Gamma Counter (PerkinElmer). A known amount of mAb1 immobilized nanoparticles in final TBST buffer (after washing and resuspending from the immobilization steps) was taken for radioactivity measurement. A stock of different known concentrations of ^{125}I labelled mAb1 in solution was taken as a control, and the radioactivity from the known amount of mAb1 functionalized nanoparticles was measured in count per second (cps), from which the immobilized mAb1 (in μg mg^{-1} of nanoparticles) was obtained. The number of immobilized mAb1 per nanoparticle was calculated initially by dividing the immobilized amount of mAb1 (in μg mg^{-1}) by the nanoparticle specific surface area (in m^2 g^{-1}); further calculating the number of antibody molecules per m^2 from antibody molecular weight, which was further translated to the number of immobilized antibodies using the average surface area per nanoparticle. The experiments were performed in triplicate and the standard deviation was calculated in each case.

In situ accessibility of immobilized antibodies on nanoparticles

In situ accessibility of Fab and Fc domains of immobilized mAb1 on nanoparticles was analyzed by two different accessibility assays. For this purpose, mAb1 immobilized nanoparticles from both sets of experiments (according to Tables S1 and S2 in the ESI†) were used in the accessibility assays to analyze the influence of immobilization conditions on accessibility.

For the Fab domain accessibility assay, a known amount of mAb1 functionalized nanoparticles was first incubated with 500 pM of cTnI solution (which is 3 molar excess of the amount of immobilized mAb1 present in solution) in PBS buffer (10 mM phosphate buffered saline, pH 7.4) for 1 h. The molar excess used was sufficient to saturate the available antibody domains, and the duration of 1 h was sufficient for the kinetics to reach a steady state, as obtained from an earlier study.[16] After incubation, the particles were quickly washed twice with PBS buffer and thereafter, the ^{125}I labelled mAb2 was added for sandwich assay binding. Similar to cTnI, around 3 molar excess of mAb2 was added (500 pM, compared to immobilized mAb1 present in solution) for the sandwich assay. After incubation for 1 h, the nanoparticle solution was washed three times with PBS and re-suspended in final 100 μl of PBS buffer for measuring the final radioactivity (cps) in a gamma counter. Similar to mAb1, stocks of different known concentrations of ^{125}I labelled mAb2 in solution were taken as a control, and the radioactivity from known amounts of mAb2 bound nanoparticles was measured in counts per second (cps). The amount of bound mAb2 in the Fab accessibility assay was then calculated by subtracting the signal of mAb1 immobilized particles from the final signal after mAb2 binding.

The Fc domain accessibility assay with the mAb1 immobilized particles was performed in a similar manner, but now with ^{125}I labelled protein G molecules. To the known amount of mAb1 immobilized nanoparticles 3 molar excess of radiolabelled protein G was directly added and incubated for

1 h. The protein G molecules can bind to the accessible Fc domains of the immobilized mAb1 on the nanoparticle surface. After incubation, the protein G bound particles were washed, re-suspended in PBS and measured in a gamma counter for the final radioactivity signal (cps). Similar to mAb2, the signal from labeled protein G was analyzed from a separate dose–response curve with different concentrations of labeled protein G; and the amount of protein G molecules bound to the nanoparticles was calculated by subtracting the signal of mAb1 immobilized particles from the final signal after protein G binding. The control experiment was performed with a known amount of non-functionalized COOH nanoparticles by incubating a similar amount of labelled mAb2 and protein G.

The net amount of radioactivity signal (cps) due to the binding of mAb2 and protein G in the accessibility assays was further converted to the amount of these biomolecules bound (in μg) per mg of nanoparticles, and subsequently to the number of biomolecules bound per nanoparticle, as described above in the case of mAb1. These accessibility assay experiments using the mAb1 immobilized nanoparticles from both the sets (ESI, Tables S1 and S2†) were performed in triplicate and the standard deviation was calculated in each case.

Results and discussion

An experiment based on the parameters outlined in Table 1 was designed with the design-of-experiment software package MODDE, with three responses: mAb1 immobilization capacity, the amount of accessible Fab domain and the amount of accessible Fc domain. A total of 19 experiments (ESI, Table S1†) were performed (including 3 replicates at center points) and the results were represented as a four-dimensional contour graph, see Fig. 1. The graph shows how the mAb1 immobilization, Fab and Fc accessibility scale (expressed as a mass ratio and as a number ratio) with the four chemical parameters. In summary, the mAb1 immobilization scales down with increased coupling pH, and scales up with added EDC and mAb1 (towards the top-left corner of Fig. 1A–C), while it is not significantly dependent on the nanoparticle surface activation pH (see also ESI Fig. S5†). The data reveal a significant impact of the coupling parameters on the immobilized amount, with variations between 2.3 μg and 47.4 μg of mAb1 per 1 mg of nanoparticle, corresponding to a calculated amount of 0.2×10^3 to 5.9×10^3 mAb1 molecules per nanoparticle. This corresponds to a range between a tenth of a monolayer and a closely packed high density surface coverage.[16,21,22] The nanoparticle surface activation pH range between 5.0 and 6.0 did not have a significant influence on the mAb1 immobilization (at a pH below 5.0, clustering of nanoparticles was observed). However, the mAb1 immobilization decreases about 2 fold upon increasing the antibody coupling buffer pH from 5.5 to 6.5. The reduced immobilization density at pH 6.5 may be caused by electrostatic repulsion between the negatively charged carboxylated surface and the deprotonated antibody molecules (the isoelectric point of the mAb1 is around pH 6.0).

The immobilized mAb1 amount scales with an increase of the molar equivalent of EDC to the available carboxyl groups from 0.5 to 2.0, which can be attributed to a higher amount of activated surface carboxyl groups. As EDC couples antibody molecules *via* their primary amine groups, a higher amount of activated surface carboxyl groups can also facilitate the formation of multiple bonds with the antibody molecules. At both higher mAb1 concentration (100 μg mg^{-1} MNP) and higher EDC concentration (EDC to carboxyl group molar ratio 2.0), a very high immobilized amount of 4000–5000 mAb1/MNP was observed (Fig. 1A, left-top corner). This amount is close to the theoretical side-on monolayer coverage on 500 nm magnetic nanoparticles.[16]

However, the influence of EDC is not significant at a coupling pH of 6.5 (Fig. 1A, right column). At elevated pH, the antibody and the particle surface acquire a stronger negative charge, so electrostatic repulsion is probably the cause of the reduced antibody immobilization density. At pH 6.5, a higher mAb1 concentration results in an increased immobilization amount from around 500 to 1000 mAb1/MNP (Fig. 1A, right column from bottom to top), but the amount remains significantly lower than at lower coupling pH (pH 5.5).

Given the immobilization strategy *via* the amine group on the antibody molecules, a heterogeneous distribution of bond formation between the antibody molecules and nanoparticle surface is expected, which raises the question about the site-specific accessibility of the immobilized antibody domains. The domain specific accessibility of the immobilized mAb1 was assessed by the mAb2 binding sandwich assay (for the Fab domain) and the protein G binding assay (for the Fc domain) as described above. The absolute amount of bound mAb2 and protein G was quantified in these assays and analyzed as a function of mAb1 immobilized conditions (contour graph, Fig. 1B and C respectively). The data show, in the entire immobilized mAb1 regime, that the accessible amounts of Fab and Fc domains were limited to a molar ratio range of around 0.2 to 0.3 of immobilized mAb1 (corresponds to the absolute amount of 0.2×10^3 to 1.0×10^3 bound mAb2 or protein G per nanoparticles, respectively). Compared to the data on the amount of mAb1 (Fig. 1A), the data on the accessibility of Fab domains (Fig. 1B) and Fc domains (Fig. 1C) show rather weak dependencies on the coupling conditions. The relative fraction of the accessible Fab and Fc domains and the dependencies on individual chemical parameters are shown in Fig. S6 and S7 in the ESI.† The Fab accessibility sensitively depends on coupling parameters. Interestingly, the left column of Fig. 1A–C (at coupling pH 5.5) shows similar dependencies in the mAb1 immobilized amount, and in the Fab and Fc domain accessibilities. In particular, these parameters all scale with the EDC concentration in a similar way.

The similar influence of immobilization conditions on the mAb1 amount and on the accessible Fab and Fc domains suggests the analysis of the site-specific accessibility as a function of the immobilized mAb1 density, as plotted in Fig. 2.

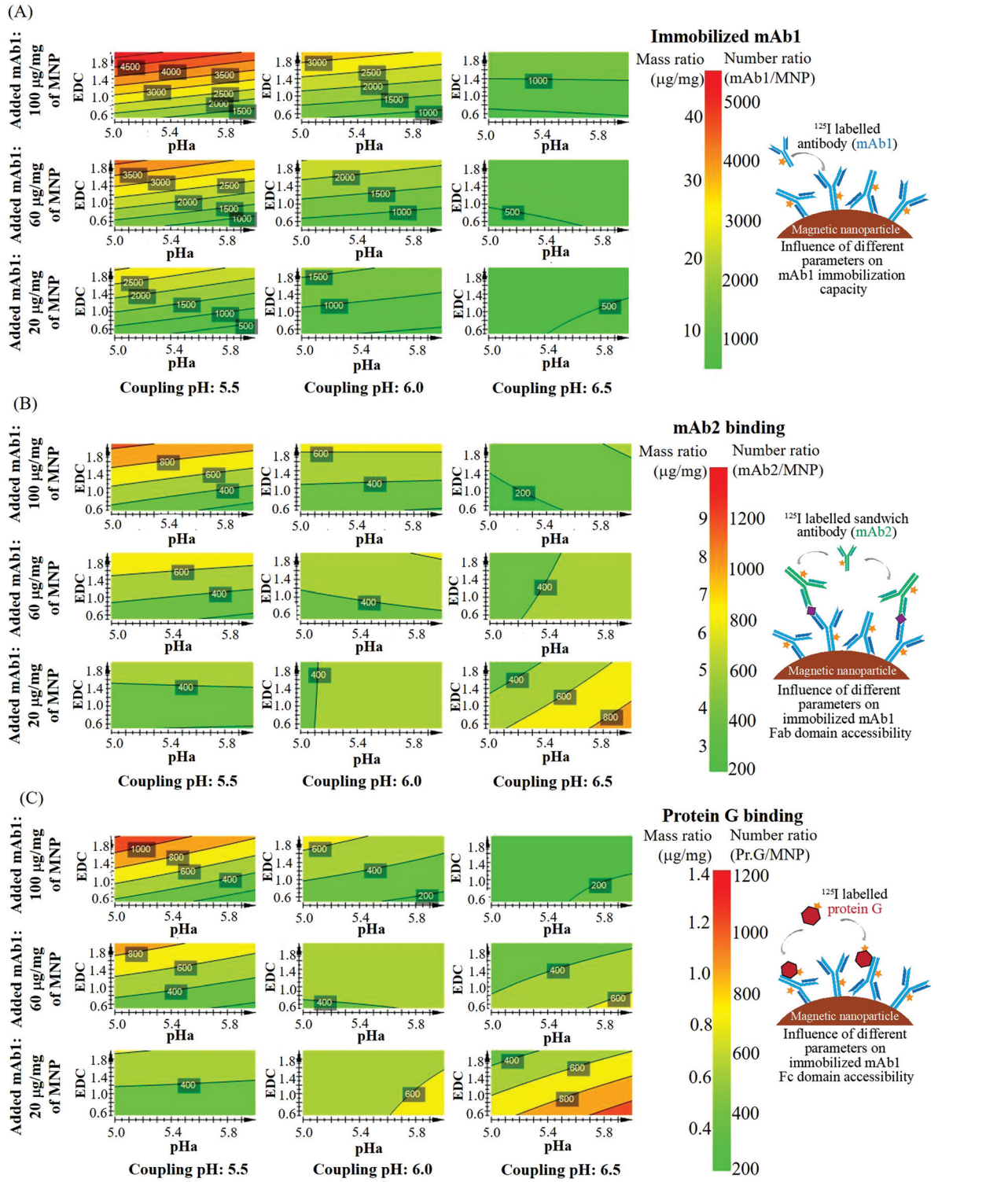

Fig. 1 Results of the experiments for different coupling parameters, presented as a 4D contour graph: (A) immobilized amount of mAb1 on magnetic nanoparticles, under different coupling conditions (cross-linker concentration, antibody concentration, activation and coupling pH). (B) Fab domain accessibility assay: amount of bound mAb2 antibodies in a cTnI sandwich assay; (C) Fc domain accessibility assay: amount of bound protein G molecules, in a direct binding assay. Accessibility assays were performed with the same set of nanoparticles used for immobilization. The scales show the amount of immobilized or bound biomolecules (*i.e.* mAb1, mAb2 or protein G) in two different units: in the number of biomolecules per nanoparticle, and in μg of biomolecules per mg of nanoparticles. All the graphs are plotted as a function of four different mAb1 coupling conditions. Primary *X* axis: nanoparticle surface activation pH (pHa), primary *Y* axis: cross-linker (EDC) added in molar equivalence of COOH groups on the nanoparticle surface (0.7 mmol of COOH groups per 1 g of nanoparticles, as specified by the supplier), secondary *X* axis: antibody coupling pH, secondary *Y* axis: amount of mAb1 added in μg per mg of nanoparticle for immobilization. The numbers are expressed as a number ratio. These plots were also validated using experimental *versus* predicted data (see ESI, Fig. S4†).

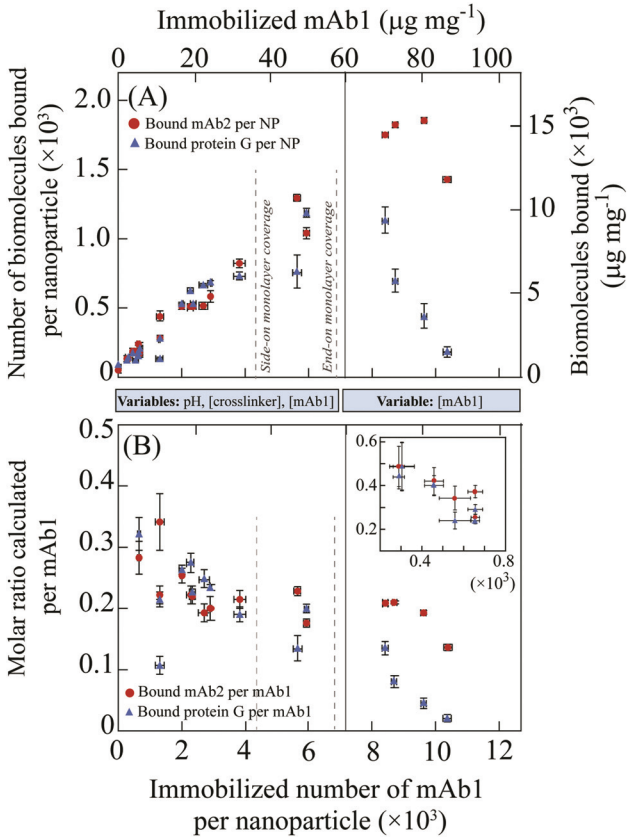

Fig. 2 Accessibility assays as a function mAb1 surface coverage: (A) absolute amount of mAb2 bound and protein G bound per nanoparticle, in a sandwich assay and in a direct assay, respectively; (B) molar ratio of bound mAb2 and protein G to immobilized mAb1 per nanoparticle, from the accessibility assays. All the data points represented here have more than 2 times higher signal than the background. Vertical dashed line (i) represents the calculated maximum monolayer coverage of immobilized mAb1 in a 'side-on' orientation; line (ii) represents the calculated maximum monolayer coverage of immobilized mAb1 in an 'end-on' orientation. The blue bars in between the graphs represent two sets of experimental data along the *x*-axis, the left bar shows the range of the data points with the particles from different mAb1 immobilization condition experiments (Table S1†), and the right bar represents the data points with the particles where only the mAb1 concentration was varied during immobilization (Table S2†). Inset B: Expanding the data points in a lower antibody surface density regime (having less than 2 times higher signal than the background), which were not considered for accessible molar ratio calculation and were not included in the main part of (B).

Here a clear correlation between the surface mAb1 density and the site-specific accessibility is observed for both the Fab and Fc domains. Fig. 2A shows that the absolute amounts of the accessible Fab and Fc domains scale linearly (from 0.2×10^3 to 1.2×10^3 molecules per MNP) with the surface mAb1 density up to the monolayer coverage (around 6.0×10^3 mAb1/MNP). Over this range, the molar ratio of accessible Fab and Fc domains gradually decreases from 0.3 to 0.2 on increasing the mAb1 amount (Fig. 2B). These values are much lower than one, which indicates that the domains targeted on the mAb1 are to a large extent inaccessible. This can be attributed to the variable orientation of the immobilized antibody molecules, due to the coupling *via* the surface exposed amine groups of the antibody. In addition, partial denaturation may play a role, caused by the covalent and non-covalent interactions between the antibodies and the nanoparticle surface.[23,24]

The site-specific accessibility assays of Fig. 2A show a level of background binding, *i.e.* a non-zero signal is measured in the absence of mAb1 on the particles, which is caused by non-specific binding in the assays. The underlying mechanism is the binding of reactants to the bare particle surface (binding of cTnI and/or radiolabelled mAb2 in the case of the Fab accessibility assay; and radiolabelled Protein G in the case of the Fc accessibility assay). This means that a molar ratio analysis (as in Fig. 2B) for accessible domains needs to be carried out with care. At a very low mAb1 surface coverage ($\leq 1.0 \times 10^3$ mAb1/MNP), the signals measured in the accessibility assays (Fig. 2A) are close to the background levels, so no reliable information about accessible Fab and Fc domains can be extracted. Therefore, the molar fraction of accessible domains is calculated and plotted (Fig. 2B) only if the measured signal in Fig. 2A is at least 2 times higher than the background signal. For illustration purposes, the inset in Fig. 2B shows the data points that were not considered for analyzing the molar ratio, and this clearly results in higher numbers; however these numbers cannot be interpreted as antibody accessibility as they contain systematic errors due to the non-specific binding.

The accessible Fab and Fc domains show a strong correlation with the mAb1 surface density from sub-monolayer to monolayer coverage, irrespective of the underlying immobilization conditions. To further investigate the limit of high mAb1 surface densities, mAb1 immobilization was performed with higher mAb1 concentrations (50–500 μg per mg of nanoparticles, which includes overlap with the mAb1 concentrations as shown in Table 1) under similar immobilization conditions. These conditions result in a surface density ranging from 4.0×10^3 to 10.1×10^3 mAb1/MNP, which goes beyond the calculated monolayer coverage of mAb1. This represents a crowded condition where molecular and conformation rearrangements of the antibody molecules occur.[24–26] The data from the accessibility assays with these mAb1 densities are plotted in the right lane ('Variable: [mAb1]') of Fig. 2A and B. The fractions of accessible Fab and Fc domains both decrease at high mAb1 surface density, but they decrease differently. The fraction of accessible Fab domains decreases from 0.2 at monolayer coverage (5.0×10^3 mAb1/MNP) to around 0.1 at higher mAb1 density (10.0×10^3 mAb1/MNP), while the fraction of accessible Fc domains decreases from 0.2 to approximately 0.05 in this regime. Broadly the data of Fig. 2 can be divided into two sections. In the first section until monolayer coverage, the accessible Fab and Fc domains behave very similarly. This demonstrates that the coupling process maintains the integrity of the antibodies, *i.e.* the coupling conditions are mild and the immobilization process is dominated by antibody–surface interactions rather than by antibody–antibody interactions. This can be understood from a single dominating coupling mechanism, namely coupling of

antibodies to the surface *via* the primary amines on the antibody, without a significant presence of antibody immobilization by other molecular mechanisms. The accessible Fab domain analysis also includes the antibodies which are partially oriented with one Fab arm available to capture the target antigen and can bind to the second antibody (mAb2) in the sandwich assay. Furthermore, the data show that the average orientation of the antibodies is not changed by the different conditions, which implies that the different parts of the antibody that conjugate to the nanoparticle surface have a similar dependence of reactivity on the chemical conditions. In the second section, beyond mAb1 monolayer coverage (>6.0×10^3 mAb1/MNP), the accessibility of Fab and Fc domains decreases, but not in an equal manner. This shows that molecular crowding has a strong effect on the antibodies and their orientation. The antibodies hinder each other's accessibility and furthermore the pertinent antibody–antibody interactions affect the orientation and maybe even the integrity of the antibodies. The fact that the Fab accessibility reduces less strongly under crowding than the Fc accessibility may be due to a steric effect, because coupling of the antibody *via* the apex of the Fc fragment (~50 kDa, outward antibody orientation, with Fab available) requires less surface area compared to an antibody that is coupled with the $F(ab')_2$ site (~110 kDa, inward antibody orientation, with Fc available). Furthermore, the binding site for protein G is at the side of the Fc domain (in between C_H2 and C_H3 domains),[27] so a crowding-induced shift of antibody orientation from side-on to end-on may severely restrict the accessibility of the protein G binding sites. Finally, the lower affinity of protein G–IgG binding ($K_D \sim 10^{-9}$–10^{-10} M) compared to cTnI–IgG binding ($K_D \sim 10^{-11}$ M) may also play a role in the stronger reduction of the Fc signals in a high mAb1 surface density regime.

In conclusion, we have studied the accessibility of antibodies for the widely used covalent immobilization method based on EDC chemistry, and we have developed two radiolabelled based assays for the precise quantification of the site-specific accessibility of the immobilized antibodies on nanoparticles over a surface density range from sub-monolayer to monolayer coverage. Although many techniques are available to quantify the antibody orientation on planar surfaces (see the Introduction section), to our knowledge this is the first report in the literature of a quantitative site-specific accessibility study of antibodies on nanoparticles as a function of immobilization conditions. Our experiments show that the coupling parameters (surface activation pH, coupling pH, EDC concentration, and antibody concentration) strongly impact the immobilization density, and that the site-specific accessibility of antibodies on the nanoparticles relates primarily to the immobilized density, irrespective of the immobilization conditions. We find that at sub-monolayer to monolayer coverage, the fraction of accessible Fab and Fc domains is quite stable with a molar ratio value between 0.2 and 0.3. At higher surface densities (beyond monolayer coverage) the accessible fractions decrease significantly and differently to around 0.1 and 0.05, for Fab and Fc domains, respectively.

At sub-monolayer surface coverages, the site-specific accessibility of antibodies is fairly constant, which implies that the immobilization process is dominated by antibody–substrate interactions with a stable well-defined chemical pathway, and that antibody–antibody interactions do not play a role. It will be interesting to test whether also other immobilization strategies lead to an accessibility of antibodies in the sub-monolayer regime that is independent of the coupling conditions. For non-directional coupling strategies (*e.g.* using biotin or azido modified antibodies for surface conjugation)[28] we expect that the same conclusion may be valid, provided that secondary immobilization mechanisms are absent, and that the immobilization conditions maintain the integrity of the antibodies. For directional coupling methods (*e.g.* using Fc domain sugar moieties for covalent conjugation, using enzymatic reduction of antibodies and thiol group mediated conjugation, using proteins having natural affinity for antibodies and then covalent-crosslinking, *etc.*)[29] the Fab and Fc accessibility may depend on the coupling conditions in case more than one coupling mechanism is effective. With properly designed and sufficiently high reactivities, also here we hypothesize that the site-specific accessibility of antibodies may be constant over a wide range of immobilization conditions, up to the surface density range where antibody crowding appears. For research and for assay development, the presented methodology gives an accurate view into the influence of coupling parameters on the density and site-specific accessibility of nanoparticle-coupled antibodies, and stresses the importance of reporting and judging nanoparticle biofunctionality as a function of quantified antibody surface density.

Author contributions

The manuscript was written through contributions of all authors. All the authors have given approval to the final version of the manuscript. The authors declare no competing financial interest.

Abbreviations

mAb1	Monoclonal anti-troponin antibody 1: used for immobilization on the nanoparticle surface;
mAb2	Monoclonal anti-troponin antibody 2: used for accessibility assay and sandwich binding to mAb1;
EDC	*N*-3-(dimethylamino)propyl-*N*-ethylcarbodimide hydrochloride;
cTnI	Cardiac troponin I (purchased as cTnI I-T-C complex).

Conflicts of interest

There are no conflicts to declare.

Acknowledgements

The authors thank ThermoFisher, Oslo, for providing the magnetic nanoparticles for this work and help in the initial part of the research. The authors also thank Dr Darren Ellis from ThermoFisher, Oslo; and many colleagues at the Philips Research and Eindhoven University of Technology for valuable support and discussion. The work of B. S. was partly funded by the European Commission through the 7th Framework Programme (FP7-MC-ITN BioMaX, project number 264737).

References

1 K. E. Sapsford, W. R. Algar, L. Berti, K. B. Gemmill, B. J. Casey, E. Oh, M. H. Stewart and I. L. Medintz, Functionalizing Nanoparticles with Biological Molecules: Developing Chemistries That Facilitate Nanotechnology, *Chem. Rev.*, 2013, **113**, 1904–2074.

2 W. R. Algar, D. E. Prasuhn, M. H. Stewart, T. L. Jennings, J. B. Blanco-Canosa, P. E. Dawson and I. L. Medintz, The Controlled Display of Biomolecules on Nanoparticles: A Challenge Suited to Bioorthogonal Chemistry, *Bioconjugate Chem.*, 2011, **22**, 825–858.

3 E. Steen Redeker, D. T. Ta, D. Cortens, B. Billen, W. Guedens and P. Adriaensens, Protein Engineering for Directed Immobilization, *Bioconjugate Chem.*, 2013, **24**, 1761–1777.

4 E. Polo, S. Puertas, M. Moros, P. Batalla, J. M. Guisán, J. M. de la Fuente and V. Grazú, Tips for the functionalization of nanoparticles with antibodies, *Methods Mol. Biol.*, 2013, **1051**, 149–163.

5 P. C. Lin, S. H. Chen, K. Y. Wang, M. L. Chen, A. K. Adak, J. R. R. Hwu, Y. J. Chen and C. C. Lin, Fabrication of Oriented Antibody-Conjugated Magnetic Nanoprobes and Their Immunoaffinity Application, *Anal. Chem.*, 2009, **81**, 8774–8782.

6 P. P. Joshi, S. J. Yoon, W. G. Hardin, S. Emelianov and K. V. Sokolov, Conjugation of Antibodies to Gold Nanorods through Fc Portion: Synthesis and Molecular Specific Imaging, *Bioconjugate Chem.*, 2013, **24**, 878–888.

7 H. Y. Song, X. Zhou, J. Hobley and X. Su, Comparative Study of Random and Oriented Antibody Immobilization as Measured by Dual Polarization Interferometry and Surface Plasmon Resonance Spectroscopy, *Langmuir*, 2012, **28**, 997–1004.

8 M. Iijima, M. Somiya, N. Yoshimoto, T. Niimi and S. Kuroda, Nano-Visualization of Oriented-Immobilized IgGs on Immunosensors by High-Speed Atomic Force Microscopy, *Sci. Rep.*, 2012, **2**, 790.

9 M. Bergkvist, J. Carlsson and S. Oscarsson, A Method for Studying Protein Orientation with Atomic Force Microscopy Using Relative Protein Volumes, *J. Phys. Chem. B*, 2001, **105**, 2062–2069.

10 H. Xu, X. Zhao, C. Grant, J. R. Lu, D. E. Williams and J. Penfold, Orientation of a Monoclonal Antibody Adsorbed at the Solid/solution Interface: A Combined Study Using Atomic Force Microscopy and Neutron Reflectivity, *Langmuir*, 2006, **22**, 6313–6320.

11 H. Xu, J. R. Lu and D. E. Williams, Effect of Surface Packing Density of Interfacially Adsorbed Monoclonal Antibody on the Binding of Hormonal Antigen Human Chorionic Gonadotrophin, *J. Phys. Chem. B*, 2006, **110**, 1907–1914.

12 H. Wang, D. G. Castner, B. D. Ratner and S. Jiang, Probing the Orientation of Surface-Immobilized Immunoglobulin G by Time-of-Flight Secondary Ion Mass Spectrometry, *Langmuir*, 2004, **20**, 1877–1887.

13 S. Puertas, P. Batalla, M. M. Moros, E. Polo, P. Del Pino, J. M. Guisán, V. Grazú, J. M. de la Fuente and J. M. Guisan, Taking Advantage of Unspecific Interactions to Produce Highly Active Magnetic Nanoparticle-Antibody Conjugates, *ACS Nano*, 2011, **5**, 4521–4528.

14 C. Parolo, A. de La Escosura-Muñiz, E. Polo, V. Grazú, J. M. de La Fuente and A. Merkoçi, Design, Preparation, and Evaluation of a Fixed-Orientation Antibody/gold-Nanoparticle Conjugate as an Immunosensing Label, *ACS Appl. Mater. Interfaces*, 2013, **5**, 10753–10759.

15 S.-L. Ho, D. Xu, M. S. Wong and H.-W. Li, Direct and Multiplex Quantification of Protein Biomarkers in Serum Samples Using an Immuno-Magnetic Platform, *Chem. Sci.*, 2016, **7**, 2695–2700.

16 B. Saha, T. H. Evers and M. W. J. Prins, How Antibody Surface Coverage on Nanoparticles Determines the Activity and Kinetics of Antigen Capturing for Biosensing, *Anal. Chem.*, 2014, **86**, 8158–8166.

17 C. Mateo, R. Torres, G. Fernández-Lorente, C. Ortiz, M. Fuentes, A. Hidalgo, F. López-Gallego, O. Abian, J. M. Palomo, L. Betancor, B. C. C. Pessela, J. M. Guisan and R. Fernández-Lafuente, Epoxy-Amino Groups: A New Tool for Improved Immobilization of Proteins by the Epoxy Method, *Biomacromolecules*, 2003, **4**, 772–777.

18 B. Tural, S. Tural, E. Ertaş, İ. Yalınkılıç and A. S. Demir, Purification and covalent immobilization of benzaldehyde lyase with heterofunctional chelate-epoxy modified magnetic nanoparticles and its carboligation reactivity, *J. Mol. Catal. B: Enzym.*, 2013, **95**, 41–47.

19 D. A. Morrow, C. P. Cannon, R. L. Jesse, L. K. Newby, J. Ravkilde, A. B. Storrow, A. H. B. Wu, R. H. Christenson, F. S. Apple, G. Francis and W. Tang, National Academy of Clinical Biochemistry Laboratory Medicine Practice Guidelines: Clinical Characteristics and Utilization of Biochemical Markers in Acute Coronary Syndromes, *Clin. Chem.*, 2007, **53**, 552–574.

20 A. van Reenen, A. M. de Jong, J. M. J. den Toonder and M. W. J. Prins, Integrated Lab-on-Chip Biosensing Systems Based on Magnetic Particle Actuation–a Comprehensive Review, *Lab Chip*, 2014, **14**, 1966–1986.

21 V. R. Sarma, E. W. Silverton, D. R. Davies and W. D. Terry, The Three-Dimensional Structure at 6 Å Resolution of a Human γG1 Immunoglobulin Molecule, *J. Biol. Chem.*, 1971, **246**, 3753–3759.

22 J. Buijs, J. W. T. Lichtenbelt, W. Norde and J. Lyklema, Adsorption of Monoclonal IgGs and Their F(ab′)2 Fragments onto Polymeric Surfaces, *Colloids Surf., B*, 1995, **5**, 11–23.
23 B. B. Langdon, M. Kastantin, R. Walder, D. K. Schwartz and I. P.-P. Associations, *Biomacromolecules*, 2014, **15**, 66–74.
24 Y.-Y. Cheng, H.-C. Chang, G. Hoops and M.-C. Su, Stabilization of Yeast Cytochrome c Covalently Immobilized on Fused Silica Surfaces, *J. Am. Chem. Soc.*, 2004, **126**, 10828–10829.
25 J. Kim and G. Somorjai, Molecular Packing of Lysozyme, Fibrinogen, and Bovine Serum Albumin on Hydrophilic and Hydrophobic Surfaces Studied by Infrared-Visible Sum Frequency Generation and Fluorescence Microscopy, *J. Am. Chem. Soc.*, 2003, **125**, 3150–3158.
26 S. Boujday, A. Bantegnie, E. Briand, P. G. Marnet, M. Salmain and C. M. Pradier, In-Depth Investigation of Protein Adsorption on Gold Surfaces: Correlating the Structure and Density to the Efficiency of the Sensing Layer, *J. Phys. Chem. B*, 2008, **112**, 6708–6715.
27 K. Kato, L. Y. Lian, I. L. Barsukov, J. P. Derrick, H. H. Kim, R. Tanaka, A. Yoshino, M. Shiraishi, I. Shimada, Y. Arata and G. C. Roberts, Model for the Complex between Protein G and an Antibody Fc Fragment in Solution, *Structure*, 1995, **3**, 79–85.
28 F. Rusmini, Z. Zhong and J. Feijen, Protein Immobilization Strategies for Protein Biochips, *Biomacromolecules*, 2007, **8**, 1775–1789.
29 Y. R. Yang, Y. Liu and H. Yan, DNA Nanostructures as Programmable Biomolecular Scaffolds, *Bioconjugate Chem.*, 2015, **26**, 1381–1395.